Supporting Information

Wang et al. 10.1073/pnas.1314863110

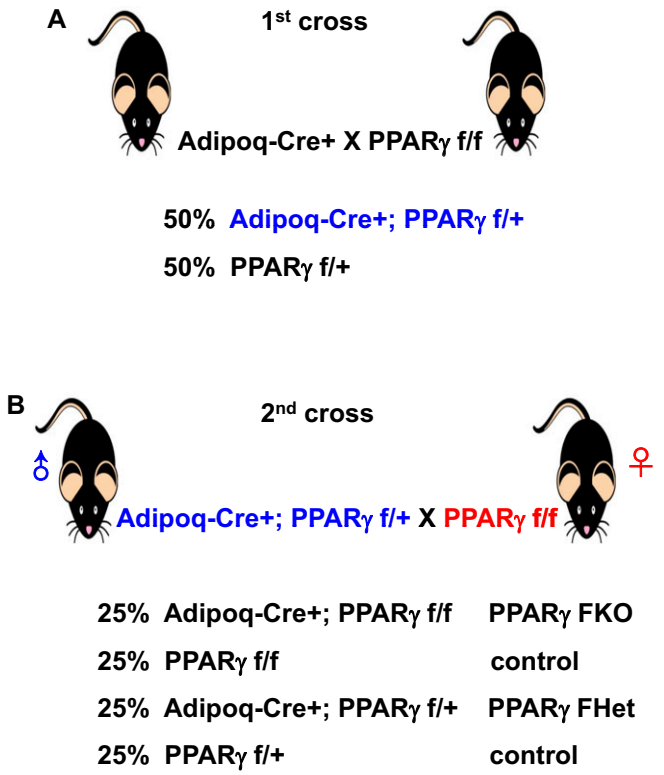

Fig. S1. Schematic of breeding strategy used to generate peroxisome proliferator-activated receptor gamma (PPARγ) fat-specific knockout (FKO) mice. (*A*) The first cross is between Adipoq–Cre+ mice and PPARγ floxed (PPARγ f/f) mice. The progeny include 50% Adipoq–Cre+; PPARγ f/+ mice. (*B*) The second cross is between male Adipoq–Cre+; PPARγ f/+ mice generated by the first breeding and female PPARγ f/f mice. Out of their progeny, 25% are PPARγ FKO (Adipoq–Cre+; PPARγ f/f), 25% are PPARγ FHet (Adipoq–Cre+; PPARγ f/+), and the rest of them are control (PPARγ f/f or PPARγ f/+) mice.

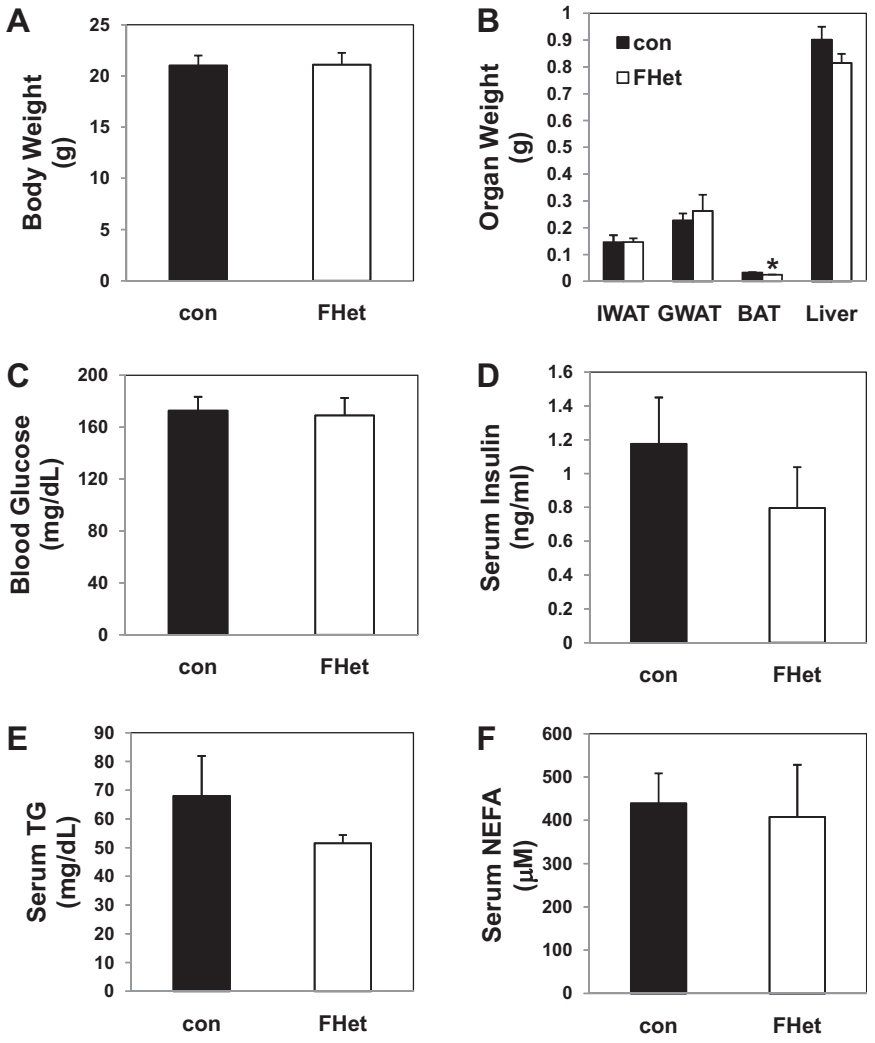

Fig. S2. No dramatic phenotype difference is observed between PPARγ FHet and control mice. (*A* and *B*) Body weight and weight of various organs [inguinal white adipose tissue (IWAT), gonadal white adipose tissue (GWAT), brown adipose tissue (BAT), and liver] of 3-mo-old female control and PPARγ FHet mice. (*C*–*F*) nonfasted blood glucose (*C*), serum levels of insulin (*D*), triglyceride (*E*), and free fatty acid (*F*) are shown for 3-mo-old female control and PPARγ FHet mice. Values are mean ± SEM ($n = 3$). *$P < 0.05$ vs. controls.

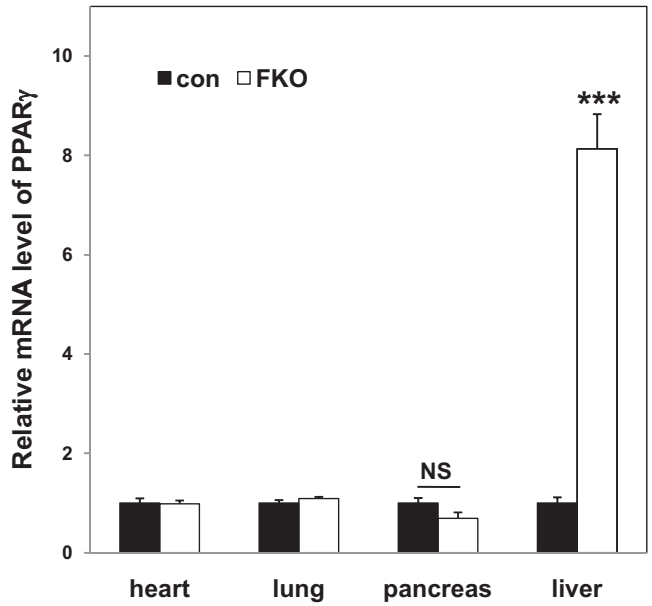

Fig. S3. PPARγ expression in heart, lung, pancreas, and liver of 3-mo-old male control and PPARγ FKO mice. Values are mean ± SEM ($n = 5$). NS, not significant; ***$P < 0.001$ vs. controls.

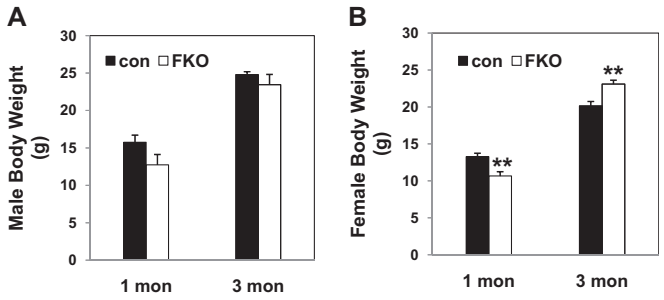

Fig. S4. Body weight of male (*A*) or female (*B*) control and PPARγ FKO mice at age 1 or 3 mo. Values are mean ± SEM ($n = 4$–8). **$P < 0.01$ vs. controls.

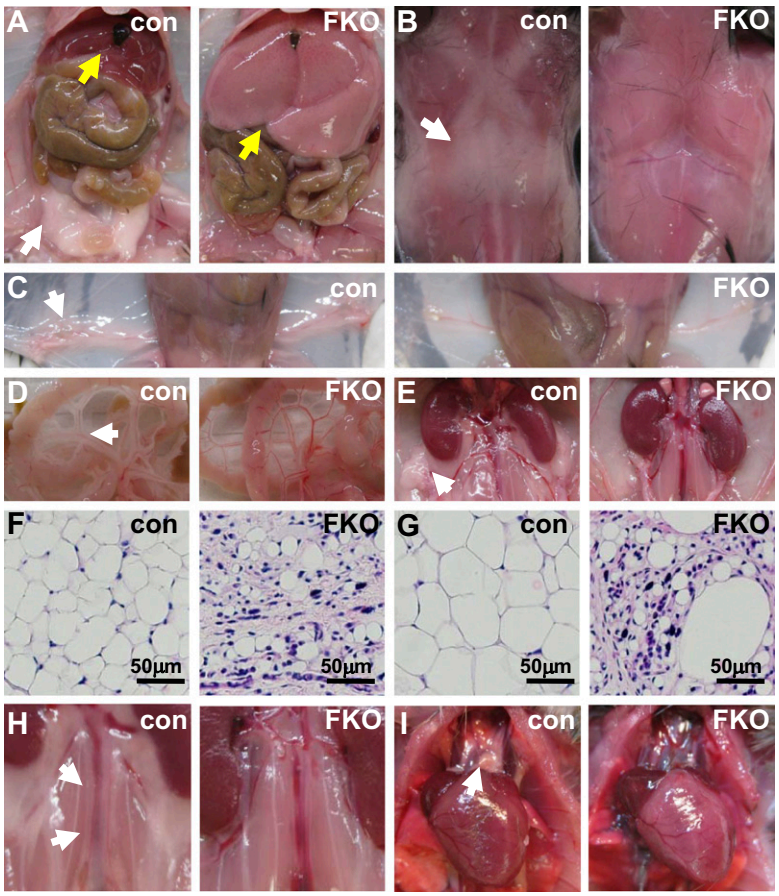

Fig. S5. Lipoatrophy in 3-mo-old female PPARγ FKO mice and Loss of perivascular and pericardial WAT in 3-mo-old male PPARγ FKO mice. (*A*–*E*) Gross morphology of GWAT (white arrow) and liver (yellow arrow) (*A*), interscapular fat (*B*), IWAT (*C*), mesenteric WAT (*D*), and perirenal WAT (*E*) from 3-mo-old female control and PPARγ FKO mice. (*F* and *G*) H&E staining of IWAT (*F*) and GWAT (*G*) from 3-mo-old female control and PPARγ FKO mice. (*H* and *I*) Photos of perivascular (*H*) and pericardial WAT (*I*) from 3-mo-old male control and PPARγ FKO mice.

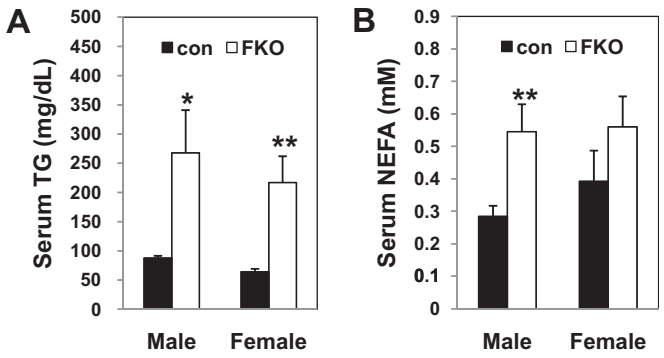

Fig. S6. Serum triglyceride (*A*) and free fatty acid (*B*) levels in male or female 3-mo-old control and PPARγ FKO mice in nonfasted state. Values are mean ± SEM ($n = 4$–6). *$P < 0.05$; **$P < 0.01$ vs. controls.

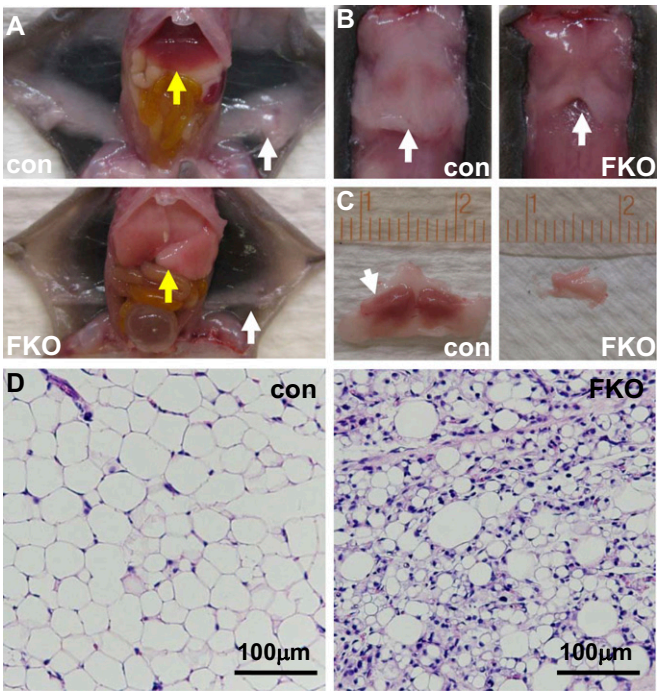

Fig. S7. WAT loss and pale liver is in 8-d-old female PPARγ FKO pups. (*A*) Exposed ventral view of liver (yellow arrows) and IWAT (white arrows) in the 8-d-old female control and PPARγ FKO pups. (*B*) Exposed dorsal view of interscapular WAT (arrows) in 8-d-old female control and PPARγ FKO mice. (*C*) Flip side of isolated interscapular fat depot in *B* from 8-d-old female control and PPARγ FKO pups, demonstrating the absence of BAT (arrow) in PPARγ FKO pups. (*D*) H&E staining of IWAT from 8-d-old female control and PPARγ FKO pups.

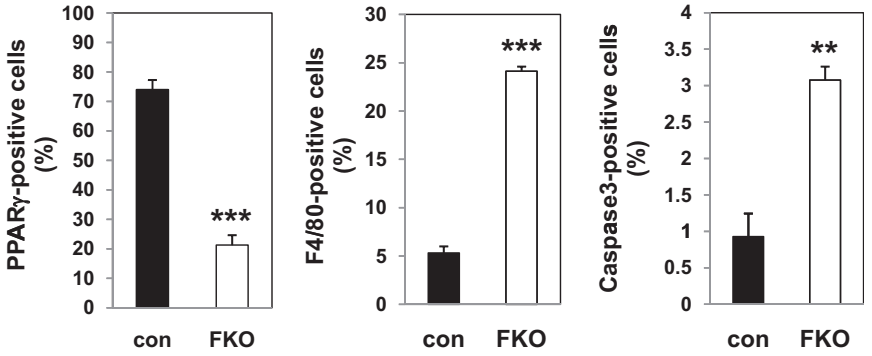

Fig. S8. Quantification of immunostaining results of IWATs from 8-d-old pups. Percentages of cells positive for the indicated immunohistochemical markers are shown. Values are mean ± SEM (n = 3–5). $^{**}P < 0.01$; $^{***}P < 0.001$ vs. controls.

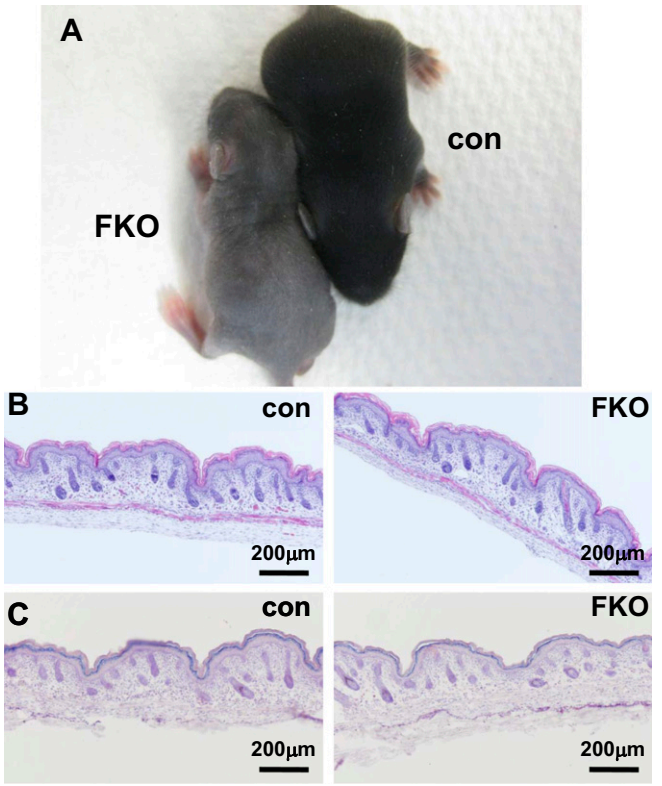

Fig. S9. Delayed hair coat formation in 8-d-old PPARγ FKO pups but no obvious alteration in skins from 1-d-old PPARγ FKO pups. (*A*) Gross coat appearance of 8-d-old control and PPARγ FKO pups. (*B* and *C*) H&E (*B*) and Oil Red O (*C*) staining sections of skins from 1-d-old male control and PPARγ FKO pups.

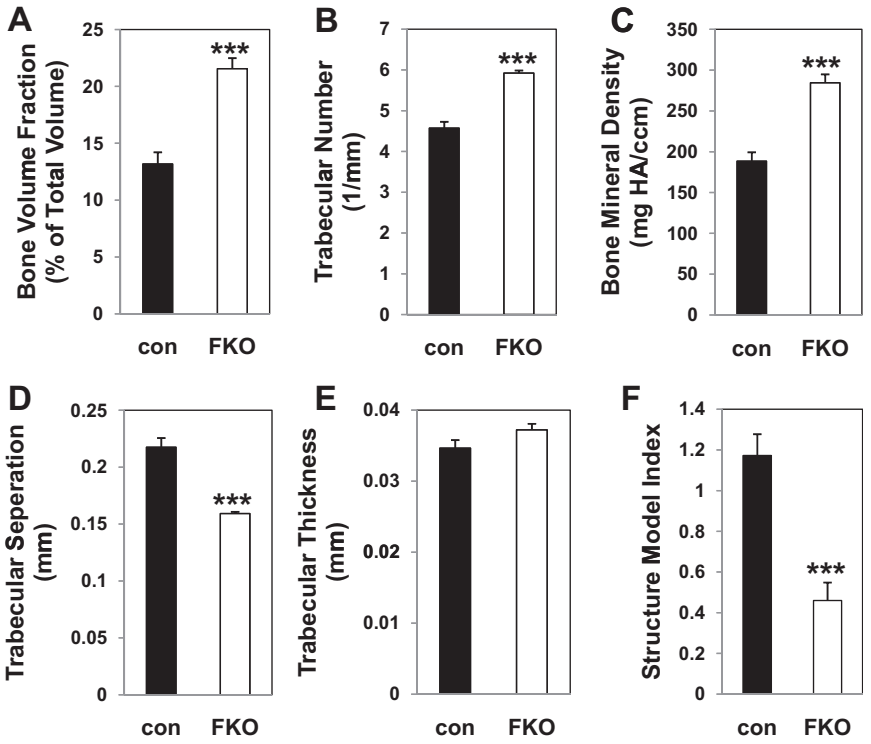

Fig. S10. Increased bone mass in 4-mo-old PPARγ FKO mice. Microcomputed tomography trabecular bone analysis of fourth lumbar vertebrae from 4-mo-old female control and PPARγ FKO mice was performed to generate various morphology parameters, including bone volume fraction (*A*), trabecular number (*B*), bone mineral density (*C*), trabecular separation (*D*), trabecular thickness (*E*), and structure model index (*F*). Values are mean ± SEM ($n = 5$). ***$P < 0.001$ vs. controls.

Table S1. Primers used for reverse transcription-quantitative PCR

Primer name	Sequence
36B4 forward	5′-CGTCCTCGTTGGAGTGACAT-3′
36B4 reverse	5′-TAGTTGGACTTCCAGGTCGC-3′
PPARγ forward	5′-TCCAGCATTTCTGCTCCACA-3′
PPARγ reverse	5′-ACAGACTCGGCACTCAATGG-3′